Modelling the Effects of Static Shear on the Undrained Cyclic Torsional Simple Shear Behavior of Liquefiable Sand

Gabriele Chiaro[1], L.I. Nalin De Silva[2] and Junichi Koseki[3]
[1]*Department of Civil and Natural Resources Engineering, University of Canterbury, Christchurch, New Zealand*
[2]*Department of Civil Engineering, University of Moratuwa, Sri Lanka*
[3]*Department of Civil Engineering, University of Tokyo, Tokyo, Japan*
[1]*E-mails*: gabriele.chiaro@canterbury.ac.nz
[2]*E-mails*: nalinds@uom.lk
[3]*E-mails*: koseki@civil.u-tokyo.ac.jp

ABSTRACT: Spanning from purely theoretical standpoint to practical applications, there is a particular interest to enhance understanding of the effects of static shear on the cyclic behavior of soil elements underneath sloped ground. To address this issue, two subsequent steps were undertaken in this study. First, a systematic laboratory investigation was carried out on Toyoura sand specimens subjected to various levels of combined static and cyclic shear stresses. Then, a new state-dependent cyclic model was developed. Since experimental findings have been exhaustively reported elsewhere, in this paper they are only briefly recalled for the benefit of comprehensiveness. Instead, the new model is presented in details and its performance is verified by simulating undrained cyclic torsional simple shear tests carried out on Toyoura sand specimens. Essentially, the model is built on an extended general stress-strain hyperbolic equation approach, in which the void ratio and stress level dependency upon non-linear stress-strain response of sand is incorporated. Besides, a novel empirical stress-dilatancy relationship is used to account for the effect of density on the stress ratio as well as to model the excess pore water pressure generation in undrained shear conditions as the mirror effect of volumetric change in drained shear conditions.

KEYWORDS: Constitutive soil model, Laboratory testing, Cyclic torsional simple shear, Static shear, Toyoura sand

1. INTRODUCTION

Due to the presence of static shear, a soil element underneath sloped ground can experience partially-reversal or non-reversal shear stress loading conditions during an earthquake (Figure 1), which can have major effects on the cyclic response of sands (Chiaro et al., 2012). Predicting in a reliable manner the complicated undrained cyclic behavior of sand within sloped ground is essential to develop effective countermeasures against liquefaction-induced slope failure. Nevertheless, this is not an easy task due to a number of key factors that need to be considered simultaneously in the analysis, such as static and cyclic shear stresses, effective mean principal stress, soil density, drainage conditions, loading conditions among others.

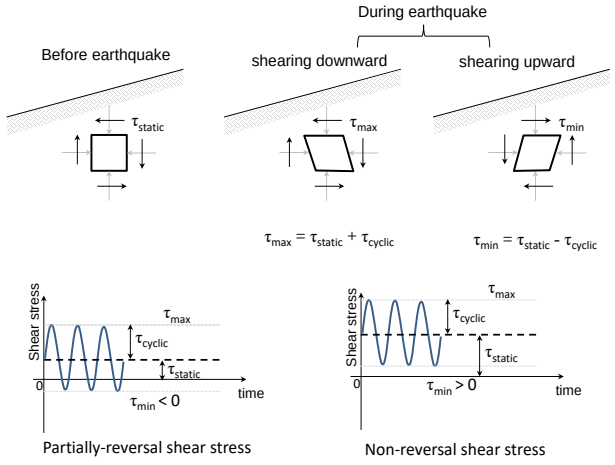

Figure 1 Shear stress in sloped ground during earthquakes

Although the importance of static shear has been widely recognized, its effects on liquefaction resistance and cyclic strength have not been fully understood yet. According to the results of cyclic triaxial tests, the presence of initial static shear may be beneficial to the liquefaction resistance (Lee and Seed, 1967; Castro and Poulus, 1977; Vaid and Chern, 1983; Hyodo et al., 1991; Vaid et al., 2001; Yang and Sze, 2011). On the contrary, laboratory tests using simple shear conditions, which provide a better representation of stress in the field during earthquake shaking, have indicated the opposite tendency, implying that resistance against liquefaction is drastically reduced by static shear existence (Yoshimi and Oh-oka, 1975; Vaid and Finn, 1979; Tatsuoka et al., 1982; Sivathayalan and Ha, 2011).

Torsional shear apparatus on hollow cylindrical specimen is recognized as an excellent tool to properly evaluate liquefaction soil response (Tatsuoka et al., 1982; Arangelovski and Towhata, 2004; Georgiannou et al., 2008). In particular, it allows reproducing the simple shear conditions (Koseki et al., 2005; Kiyota et al., 2008). Accordingly, with the aim of addressing the uncertainty before mentioned, Chiaro et al. (2012, 2013*a*) performed a number of cyclic undrained torsional simple shear tests with initial static shear on medium dense (D_r = 44-48%). It was confirmed that the presence of initial static shear does not always lead to a monotonic change in the resistance against liquefaction or more strictly to cyclic strain accumulation. In fact, it can either increase of decrease due to the magnitude of combined shear stress, the type of loading, the failure behavior and the extent of shear strain level at which the resistance against strain accumulation is defined.

Following the experimental work, Chiaro et al. (2013*b*, 2013*c*; 2015) presented a model that deals with state-dependency upon drained/undrained behavior of sand, using the generalized hyperbolic equation (GHE) approach (Tatsuoka and Shibuya, 1992) combined with an empirical linear stress-dilatancy equation valid for torsional shear conditions (Nishimura and Towhata, 2004). Such model was able to predict sand behavior in monotonic undrained torsional shear tests over a wide range of void ratios and confining pressures using a single set of soil parameters.

Using similar approach, De Silva et al. (2015) successfully simulated the cyclic drained and undrained torsional shear behavior of sand using the GHE method combined with a modified Masing's rule (Tatsuoka et al., 2003) and a bi-linear empirical stress-dilatancy relationship (De Silva et al., 2014). However, neither the density nor the combined influence of density and stress level was considered as a variable. To be precise, sand with different densities was regarded as different material and the effects of confining pressure were considered to be independent from the density state. As a

consequence, a number of soil parameters were needed for simulating different density and stress level conditions.

Taking advantages from these experimental and numerical achievements, this paper aims at developing a useful tool that may help practicing engineers and researchers to predict the cyclic response of saturated sandy soils in sloped ground experiencing both partially-reversal and non-reversal loading conditions, over a wide range of densities and stress conditions. In this context, by extending and combining both the former monotonic state-dependent model by Chiaro et al. (2013*b*, 2013*c*; 2015) and the drained/undrained cyclic model by De Silva et al. (2015), a state-dependent cyclic model which makes it possible to simulate the effects of initial static shear on the undrained cyclic behavior of saturated sand is presented. The main advantage of the proposed model is the use of limited number of soil parameters, which have a clear physical meaning and can be straightforwardly determined in the laboratory. Applicability of the proposed model is verified by simulating some of the test results presented by Chiaro et al. (2012, 2013*a*).

2. STRESSES AND STRAINS IN TORSIONAL SHEAR TESTS ON HOLLOW CYLINDER SPECIMENS

In using a hollow cylinder torsional shear apparatus, four independently loading components, namely vertical axial load (F_z), torque load (T), inner cell pressure (p_i) and outer cell pressure (p_o) can be applied (Figure 2). The correspondent stress components i.e. axial stress (σ_z), radial stress (σ_r), circumferential stress (σ_θ) and torsional shear stress ($\tau_{z\theta}$) can be defined as follows (Hight et al., 1983):

$$\sigma_z = \frac{F_z}{\pi(r_o^2 - r_i^2)} + \frac{(p_o r_o^2 - p_i r_i^2)}{(r_o^2 - r_i^2)} \tag{1}$$

$$\sigma_r = \frac{(p_o r_o + p_i r_i)}{(r_o + r_i)} \tag{2}$$

$$\sigma_\theta = \frac{(p_o r_o - p_i r_i)}{(r_o - r_i)} \tag{3}$$

$$\tau = \tau_{z\theta} = \frac{3T}{2\pi(r_o^3 - r_i^3)} \tag{4}$$

where r_o and r_i are the outer and inner radius of the specimen, respectively.

Moreover, the average torsional shear strain is defined as:

$$\gamma = \gamma_{z\theta} = \frac{2\theta}{3H}\frac{(r_o^3 - r_i^3)}{(r_o^2 - r_i^2)} \tag{5}$$

where θ is the circumferential angular displacement and H is the specimen height.

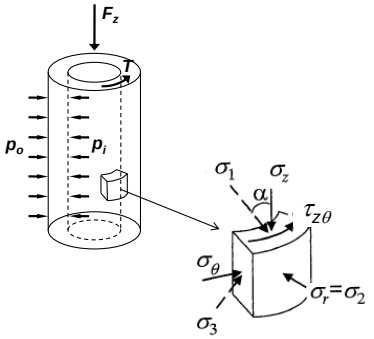

Figure 2 External forces and stress components acting on a hollow cylindrical specimen (Chiaro et al., 2013*b*)

The average principal stresses σ_1 (major), σ_2 (intermediate), σ_3 (minor) as well as the mean principal stress p are given by:

$$\begin{Bmatrix}\sigma_1\\ \sigma_3\end{Bmatrix} = \frac{\sigma_z + \sigma_\theta}{2} \pm \sqrt{\left(\frac{\sigma_z - \sigma_\theta}{2}\right)^2 + \tau_{z\theta}^2} \tag{6}$$

$$\sigma_2 = \sigma_r \tag{7}$$

$$p = \frac{\sigma_1 + \sigma_2 + \sigma_3}{3} \tag{8}$$

3. STATE-DEPENDENT CYCLIC MODEL FOR SANDS

3.1 Modelling the cyclic torsional stress-strain response

Following the classical elasto-plastic theory, in the proposed model, torsional shear strain increment (dγ) is defined as the sum of elastic torsional shear strain increment (dγ^e) and plastic torsional shear strain increment (dγ^p):

$$d\gamma = d\gamma^e + d\gamma^p \tag{9}$$

Nevertheless, it is assumed that for any given torsional shear stress increment (dτ) both elastic and plastic torsional shear deformation do always occur, so that sand continuously yields from the very small strains and a purely elastic region does not exist.

The highly non-linear stress-strain behavior of sand subjected to drained/undrained shearing can be modeled by using a Generalized Hyperbolic Equation (GHE; Tatsuoka and Shibuya, 1992). Typically, GHE is in the form of:

$$y = \frac{x}{\frac{1}{\xi_1(x)} + \frac{x}{\xi_2(x)}} \tag{10}$$

where x and y are two functions representing normalized plastic shear strain and shear stress, respectively:

$$y = \frac{\tau}{\tau_{max}} \quad \text{(original GHE)} \tag{11a}$$

$$x = \gamma^p \frac{G_{max}}{\tau_{max}} \text{ (original GHE)} \tag{11b}$$

where γ^p is the plastic torsional shear strain; τ and τ_{max} are the current and the maximum torsional shear stresses, respectively; and G_{max} is the small strain stiffness.

In the GHE proposed by Tatsuoka and Shibuya (1992), $\xi_1(x)$ and $\xi_2(x)$ are two fitting parameters varying with the shear strain level, necessary to simulate in a more realistic manner the highly complex non-linear stress-strain behavior of sand. In this paper, for the case of torsional shear loading, they were formulated as follows:

$$\xi_1(x) = \frac{1+\psi_\alpha}{2}\xi_1(0) + \frac{1-\psi_\alpha}{2}\xi_1(\infty) \tag{12a}$$

$$\xi_2(x) = \frac{1+\psi_\beta}{2}\xi_2(0) + \frac{1-\psi_\beta}{2}\xi_2(\infty) \tag{12b}$$

$$\psi_\alpha = \cos\left\{\frac{\pi}{(\alpha/x)^\Gamma + 1}\right\};\ \psi_\beta = \cos\left\{\frac{\pi}{(\beta/x)^\Gamma + 1}\right\} \tag{12c}$$

where $\xi_1(0)$, $\xi_1(\infty)$, $\xi_2(0)$, $\xi_2(\infty)$, α, β, Γ are model parameters obtained by fitting the experimental data plotted in terms of y/x vs. y relationship, as typically shown in Figure 3. Specifically, $\xi_1(0)$ is the initial normalized plastic shear modulus and $\xi_2(\infty)$ represents the normalized peak strength of soil.

From the analysis of a number of torsional shear tests, De Silva et al. (2015) demonstrated that, if properly normalized, the stress-strain relationship of sand can be represented by a unique curve irrespective of density, stress level and drainage conditions. Accordingly, the following *x* and *y* functions can be used to account for the void ratio and the effective mean principal stress dependence of drained/undrained stress-strain behavior of sand into the GHE (Chiaro et al., 2013*b;* 2015):

$$y = \frac{\tau / p'}{(\tau / p')_{\max}} \text{ (extended GHE)} \qquad (13a)$$

$$x = \gamma^{p} \frac{G_0 / p_0'}{(\tau / p')_{\max}} \text{ (extended GHE)} \qquad (13b)$$

where γ^p is the plastic torsional shear strain; τ is the torsional shear stress; p' and p_0' are the current and initial effective mean principal stresses, respectively; $(\tau/p')_{max}$ is the torsional peak shear stress ratio in the plot τ/p' vs. γ^p; and G_0 is the initial shear modulus. Note that in Eqns. (13*a)* and (13*b*), the dependence of void ratio (e_0) and stress level (p_0') is accounted by both G_0 and $(\tau/p')_{max}$, which are two parameters with clear physical meaning.

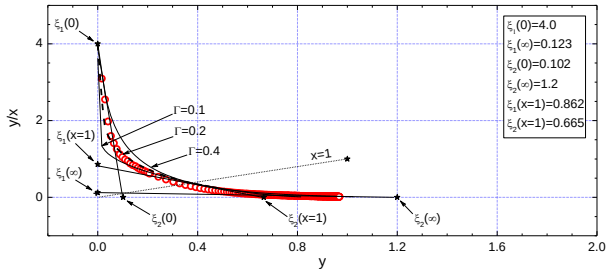

Figure 3 Evaluation of GHE soil parameters

For clean sands, a number of empirical relationships have been proposed to relate G_0 to the confining pressure and void ratio (Hardin and Richart, 1963; Iwasaki et al., 1978). Above all, for the case of sand subjected to torsional shear loading, the following expression is valid (Kiyota et al., 2006):

$$G_0 = G_n \, f(e_0)(p_0'/p_a)^n \qquad (14)$$

where G_n is the shear modulus at the reference atmospheric pressure (p_a = 100kPa) and n is a soil parameter to express the stress-level dependence of G_0. Note that in this model, $f(e_0)$ is the void ratio function for sand with round particles as proposed by Hardin and Richart (1963):

$$f(e_0) = \frac{(2.17 - e_0)^2}{1 + e_0} \qquad (15)$$

On the other hand, based on the results of monotonic undrained torsional shear tests on Toyoura sand specimens, Chiaro et al. (2013*b*, 2015) suggested that there exists a linear dependency between the peak strength and the void ratio:

$$(\tau / p')_{\max} = \rho_1 - \rho_2 e_0 \qquad (16)$$

where ρ_1 and ρ_2 are soil strength constants.

In the model, the elastic torsional shear strain increment ($d\gamma^e$) is calculated as formulated in the quasi-elastic constitutive model proposed by HongNam and Koseki (2005):

$$d\gamma^e = d\tau / G \qquad (17)$$

$$G = G_{ic} \frac{f(e)}{f(e_{ic})} \left(\frac{p'}{p_{ic}'} \right)^n \qquad (18)$$

where G is the current elastic shear modulus; $f(e)$ is the current void ratio function as defined in Eq. (15); $f(e_{ic})$ is the void ratio function at a reference isotropic confining stress p_{ic}'; G_{ic} is the initial elastic shear modulus at e_{ic} and p_{ic}'; and n is the same material parameter used in Eq. (14).

Similarly to the experimental procedure, the presence of initial static shear stress is introduced in the model by simulating a monotonic drained torsional shear loading path before the undrained one. As shown in Figure 4, the *x*-*y* relationships from drained to undrained (two-phase stress-strain path) shows a continuity of strain development during the change of loading from drained to undrained. This make it possible to model the entire two-phase monotonic loading curve by employing Eqns. (4) and (5) with a single set of GHE parameters.

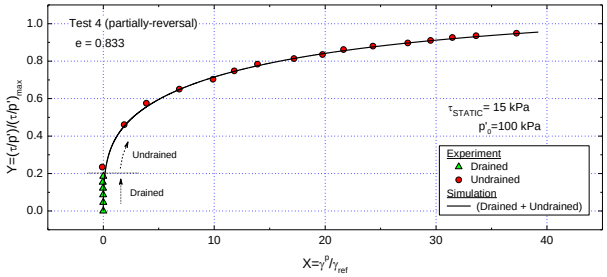

Figure 4 Measured and simulated two-phase skeleton curve

It is recognized that, cyclic behavior of soil can be modeled by employing the well-known 2nd Masing's rule. However, due to rearrangement of particles, soil behavior does not necessary follow the original Masing's rule during cyclic loadings (Tatsuoka et al., 1997). This feature can be taken into account by dragging the corresponding skeleton curve in opposite direction to the loading path by an amount δ while applying the Masing's rule (Masuda et al., 1999; Tatsuoka et al., 2003). In this study the following drag function proposed by HongNam (2004) is used:

$$\delta = \frac{x'}{\frac{1}{F_1} + \frac{x'}{F_2}} \qquad (19)$$

where F_1 is the maximum amount of drag; F_2 is a fitting parameter, which is equivalent to the initial gradient of the drag function; and x' = $\Sigma\Delta x$, where Δx denotes the increment of normalized plastic shear strain.

However, it was observed by De Silva and Koseki (2012) that the application of drag alone is not sufficient for simulating the cyclic stress–shear strain relationship close to the peak stress of the material. Accordingly, De Silva et al. (2015) introduced two conceptual factors to take into account for the damage (D) of plastic shear modulus at large stress level and the hardening (H) of the material during cyclic loading:

$$D = \frac{G^p}{G^p{}_{ini}} = \frac{1.45(1 - D_{ult})}{1 + \exp\left(\Sigma \left| \Delta\gamma^p \right|_p - 0.8 \right)} + D_{ult} \qquad (20)$$

where D_{ult} is the minimum value of D; $\Sigma|\Delta\gamma^p|_p$ is the torsional plastic shear strain accumulated between the current and the previous turning points;

$$H = 1 + \frac{H_x}{\frac{F_2}{F_1} + \frac{H_x}{H_{ult} - 1}} \qquad (21)$$

in which H_x is the $\Sigma\Delta|x|$ up to current turning point; H_{ult} is the maximum value of H after applying an infinite number of cycles; F_1 and F_2 are the same parameters used in the drag function.

Finally, after introducing drag, damage and hardening effects, the skeleton curve during cyclic loading is modelled as follows:

$$y = \frac{x-\delta}{\frac{1}{D\,\xi_1(x-\delta)} + \frac{|x-\delta|}{H\,\xi_2(x-\delta)}} \tag{22}$$

3.2 Stress-dilatancy relationship for cyclic torsional simple shear conditions

Volume change in drained shear tests can be considered as the mirror image of pore water pressure build-up during undrained shear tests. Change of volumetric strain in different stages of shear loading can be described by the stress-dilatancy relationship, which relates the dilatancy ratio ($-d\varepsilon^p_{vol}/d\gamma^p$) to the stress ratio ($\tau/p'$) (e.g. Pradhan et al., 1989; Shahnazari and Towhata, 2002). Nevertheless, theoretical stress-dilatancy relations, such as Rowe's equations (Rowe, 1962), are not directly applicable to the case of torsional shear loading. However, the results from torsional shear tests suggest that unique relationships between $-d\varepsilon^p_{vol}/d\gamma^p$ and τ/p' exist either for loading ($d\gamma^p > 0$) and unloading ($d\gamma^p < 0$) conditions (Pradhan et al., 1989; De Silva et al., 2014). Nishimura and Towhata (2004) recommended an empirical bi-linear stress-dilatancy relationship for sands undergoing cyclic torsional shear loading, which De Silva et al. (2014) amended to account for the damage (D) of plastic shear modulus, as quantified in Eqn. (20):

$$-\frac{d\varepsilon^p_{vol}}{d\gamma^p} = \frac{1}{D\,N_d}\left[\frac{\tau}{p'} \pm \frac{(\tau/p')_{PTL}}{D}\right] \tag{23}$$

In the above, N_d is a soil dilatancy parameter and $(\tau/p')_{PTL}$ is the stress ratio at the phase transformation (i.e. zero dilatancy state; Ishihara et al., 1975). Specifically, N_d is a density dependent parameter (Chiaro et al., 2013*b*), such as the denser the soil, the greater the N_d (Figure 5):

$$N_d = d_1 - d_2\, e_0 \tag{24}$$

where d_1 and d_2 are two parameters to express the dependence of N_d on density.

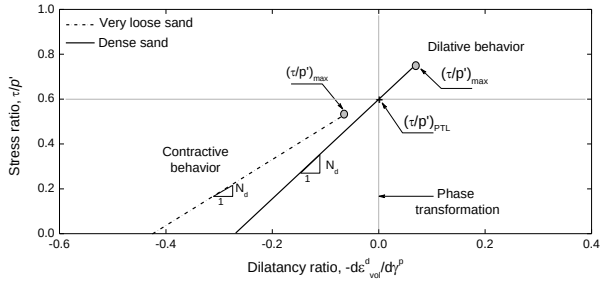

Figure 5 Schematic of stress-dilatancy relationships for sand subjected to torsional simple shear

It is well-established that, during cyclic loadings, the effective mean principal stress (p') decreases with number of cycles due to two possible mechanisms: (i) the soil is subjected to significant effects of over-consolidation until the stress state exceeds for the first time the phase transformation stress state (i.e., the first time where the volumetric behavior changes from contractive to dilative, $dp' > 0$); and (ii) soil enters into the stage of cyclic mobility. In particular, the over-consolidation significantly alters the stress-dilatancy behavior of sand during the virgin loading and its effect evanishes with the subsequent cyclic loading. Oka et al. (1999) suggested a distinct stress-dilatancy equation to reproduce the effect of over-consolidation within certain boundaries. Following the same approach, later De Silva et al. (2014, 2015) proposed the following stress-dilatancy relationship for the case of torsional shear loading:

$$-\frac{d\varepsilon^p_{vol}}{d\gamma^p} = \frac{1}{N_d}\left[\frac{\tau}{p'} \pm \frac{\tau/p'}{\ln(p_0'/p')}\right]\left[\frac{\tau/p'}{(\tau/p')_{PTL}\ln(p_0'/p')}\right]^{3/2} \tag{25}$$

In the current study, a further modification of the Eqn. (25), which consists of a rotation of over-consolidation (OC) boundary surface as schematically illustrated in Figure 6, was made to account for the combined effects of over-consolidation and initial static shear stress (τ_{static}) on undrained cyclic torsional shear behavior of sand. To this purpose, the following stress-dilatancy equation is proposed to define an anisotropic over-consolidation boundary surface (AOC):

$$-\frac{d\varepsilon^p_{vol}}{d\gamma^p} = \frac{1}{N_d}\left[\frac{\tau}{p'} \pm \frac{\tau/p' - SSR}{\ln(p_0'/p')}\right]\left[\frac{\tau/p' - SSR}{(\tau/p')_{PTL}\ln(p_0'/p')}\right]^{3/2} \tag{26}$$

$$SSR = \tau_{static}/p_0' \tag{27}$$

Note that, whenever $SSR = 0$ (i.e. $\tau_{static} = 0$), Eqn. (26) meets Eqn. (25). The proposed AOC has the same features of the one presented by Oka et al. (1999) for isotropically consolidated sands, in the sense that, it defines the region within which the specimen behaves as less contractive while being affected by over-consolidation. As well, it takes into account the effects of anisotropic consolidation induced by the static shear stress, following the same principle of the rotation of yield surface in the stress space due to anisotropic consolidation (e.g. Taiebat and Dafalias, 2010).

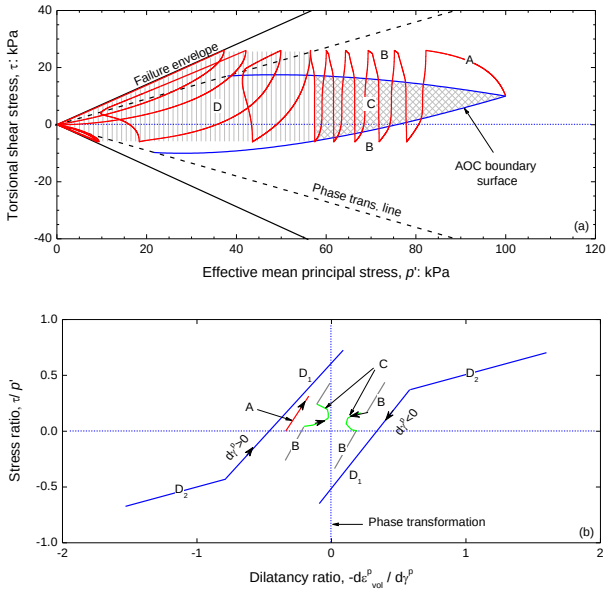

Figure 6 Schematic of (a) four-section effective stress path and (b) four-phase stress-dilatancy relationships in torsional simple shear

3.3 Four-phase dilatancy relationship

Similarly to De Silva et al. (2015), in the proposed model, the effective stress path during undrained loading is divided into four sections (Figure 6*a*) namely: (A) virgin stress path; (B) stress path within the limits of phase transformation stress state, but outside the OC boundary surface; (C) stress path within the limits of OC boundary surface, but before exceeding the phase transformation

line (PTL) for the first time; and (D) stress path after exceeding the PTL for the first time. Schematic illustration of employed four-phase dilatancy-relationship is shown in Figure 6*b*.

3.4 Modelling the excess pore water pressure generation

Excess pore water generation for saturated undrained shear conditions can be computed from volume compatibility as follows (Byrne, 1991):

$$d\varepsilon_{vol} = d\varepsilon^{e}_{vol} + d\varepsilon^{p}_{vol} \quad (28)$$

where $d\varepsilon_{vol}$ is the total volumetric strain increment, $d\varepsilon^{e}_{vol}$ is the elastic volumetric strain increment, and $d\varepsilon^{p}_{vol}$ is plastic strain increment. Such volumetric strains are the result of a change of effective mean principal stress (dp') during undrained loading that causes re-compression/swelling of the specimen, and a change of shear stress ($d\tau$) that causes the dilatation of the specimen.

For simple shear conditions, the elastic volumetric strain increment can be defined as:

$$d\varepsilon^{e}_{vol} = \frac{dp'}{K} \quad (29)$$

in which K is the bulk modulus.

Assuming that $d\varepsilon_{vol} \approx 0$ in undrained shearing tests, Eqn. (28) yields:

$$d\varepsilon^{e}_{vol} = -d\varepsilon^{p}_{vol} \quad (30)$$

Experimental evidences suggest that K can be expressed as a unique function of p':

$$K = K_{ic}\frac{f(e)}{f(e_{ic})}\left(\frac{p'}{p_{ic}'}\right)^{m} \quad (31)$$

where K_{ic} is the bulk modulus at reference effective mean stress (p_{ic}'); $f(e)$ and $f(e_{ic})$ are the void ratio function at current and reference stress state, respectively; and m is a coefficient to model the stress-state dependency of K.

Considering that $f(e) = f(e_{ic})$ in undrained tests, from Eqns. (29). (30) and (31), the change of effective means stress (i.e. generation of pore water pressure) during undrained shearing can be evaluated as:

$$dp' = K_0\left(\frac{p'}{p_0'}\right)^{m}\left(-d\varepsilon^{p}_{vol}\right) \quad (32)$$

where from Eqn. (23):

$$-d\varepsilon^{p}_{vol} = \frac{1}{D\,N_d}\left[\frac{\tau}{p'} \pm \frac{(\tau/p')_{PTL}}{D}\right]d\gamma^{p} \quad (33)$$

Similarly to G_0, also the initial bulk modulus (K_0) may be evaluated by an empirical relationship that considers the effects of initial pressure level (p_0') and void ratio (e_0):

$$K_0 = K_m\, f(e_0)(p_0'/p_a)^{m} \quad (34)$$

where K_m is a soil compressibility parameter and m is a soil parameter to express the stress-level dependence of K_0.

4. MODEL PARAMETERS

The proposed model requires a unique set of 20 parameters for simulating monotonic/cyclic drained/undrained torsional simple shear behavior of saturated Toyoura sand over a wide range of void ratios and confining pressures. The model parameters for Toyoura sand are summarized in Table 1. Due to page limitation, model calibration is not reported in this paper. However, one can refer to Chiaro et al. (2013*b*) and De Silva et al. (2015) for full details.

Table 1 Model parameters for Toyoura sand

GHE stress-strain function						
$\xi_{1(0)}$	$\xi_{1(\infty)}$	$\xi_{2(0)}$	$\xi_{2(\infty)}$	α	β	Γ
4.0	0.123	0.102	1.2	0.01073	0.85012	0.2
Shear modulus and peak shear strength						
G_n (kPa)		n		ρ_1		ρ_2
81969		0.51		1.828		-1.406
Dilatancy and bulk modulus						
d_1	d_2	$(\tau/p')_{PTL}$		K_m (kPa)		m
5.793	-5.0	0.6		47710		0.5
Drag, damage and hardening						
F_1		F_2		D_{ult}		H_{ult}
0.5		12		0.6		1.15
Four-phase dilatancy						
Phase	***Eqn.***	τ_{PTL}		N_d		***D***
A	23	0.6		Eqn. (24)		1
B	23	0.45		2.2		1
C	26	0.45		2.2		1
D_1	23	0.36		2.2		Eqn.(20)
D_2	23	0.18		0.33		Eqn.(20)

5. SIMULATION OF TEST RESULTS

As previously mentioned, as a part of a broader research study to clarify the role that static shear plays on the liquefaction and large deformation behavior of saturated sand during undrained cyclic shear loading, a systematic laboratory investigation was carried out on Toyoura sand specimens subjected to various levels of combined initial static shear and cyclic shear stress (Chiaro et al., 2012; 2013*a;* Umar et al., 2016). For completeness and to support the numerical work, in this paper the employed testing procedure and typical test results are briefly recalled hereafter.

Medium dense Toyoura sand specimens (e_0 = 0.819-0.833 corresponding to D_r = 46±2%) having the dimension of 150 mm in outer diameter, 90 mm in inner diameter and 300 mm in height, were prepared by the air pluviation method, following the procedure proposed by De Silva et al. (2006). The specimens were isotropically consolidated to an effective mean principal stress of p_0' = 100 kPa with a back pressure of 200 kPa, and then monotonically sheared by keeping drained conditions, in order to apply a specific value of initial static shear. Finally, undrained torsional shear loading was applied to simulate seismic conditions. Cyclic loading tests were performed over a wide range of initial static shear (τ_{static}) from 0 to 25 kPa. Two levels of cyclic shear stress amplitude (τ_{cyclic}), 16 and 20 kPa, were employed in order to consider various combinations of initial static and cyclic shear stress. Importantly, during the process of undrained cyclic torsional loading the vertical displacement of the top cap was prevented with the aim to simulate as much as possible the simple shear condition that ground undergoes during horizontal seismic excitation. Partially-reversal and non-reversal shear stress conditions (Figure 1) were employed and typical tests results and their numerical simulations are presented in Figures 7 to 14. It should be noted that all model predictions are obtained using the single set of model parameters reported in Table1.

5.1 Liquefaction and large cyclic post-liquefaction deformation under partially-reversal stress loading

Figures 7*a* and 8*a* show typical behavior of a medium dense Toyoura sand specimen (D_r = 45.5% or e_0 = 0.826) subjected to partially-reversal torsional simple shear loading with τ_{static} = 5 kPa and τ_{cyclic} = 16 kPa. In this test, excess pore water pressure (Δu)

generation beside a near zero shear strain development ($\gamma \approx 0$) is observed until the full liquefaction state is reached at p'= 0 kPa (i.e. $\Delta u/p$'= 100%). After this point (i.e. post-liquefaction state), rapid development of double amplitude shear strain exceeding 7.5% is clearly observed. As shown in Figures 7*b* and 8*b*, such behavior of Toyoura sand is well captured by model simulations in terms of both effective stress path and stress-strain relationship.

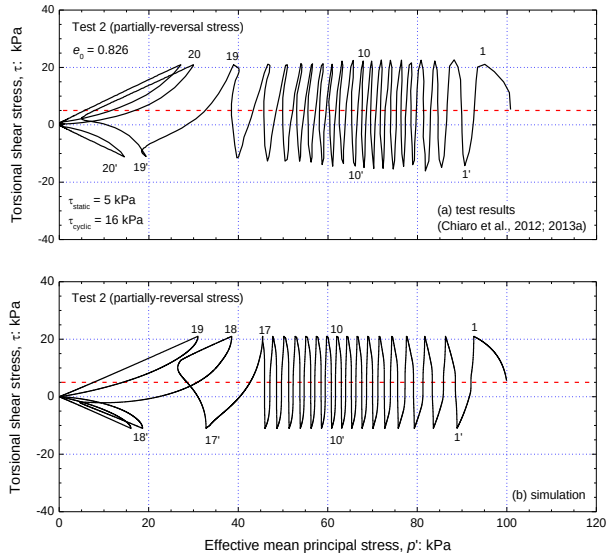

Figure 7 Measured and simulated effective stress paths for Test 2

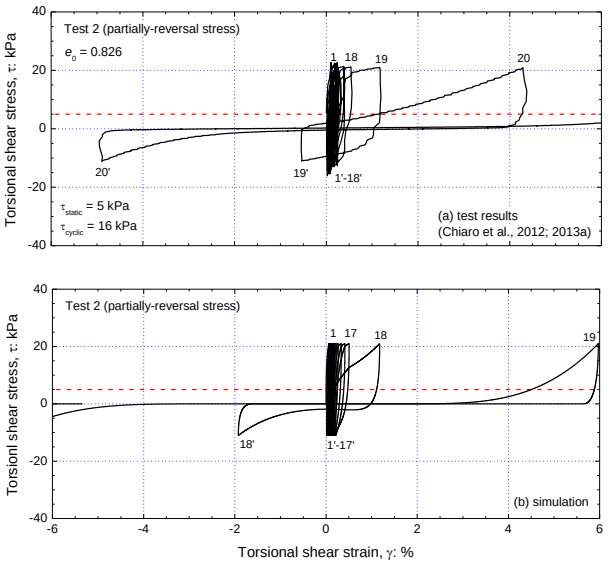

Figure 8 Measured and simulated stress-strain relationships for Test 2

5.2 Rapid liquefaction-induced large shear strain under partially-reversal stress loading

On the other hand, in the partially-reversal torsional shear test (D_r = 44.4%; e_0 =0.832; τ_{static} = 15 kPa and τ_{cyclic} = 20 kPa) shown in Figures 9*a* and 10*a*, liquefaction ($\Delta u/p$'= 100%) and rapid development of large double amplitude shear strain exceeding 7.5% took place in less than 1 cycle of loading. As displayed in Figures 9*b* and 10*b*, also such abrupt behavior of Toyoura sand is well described by model simulations in terms of both effective stress path and stress-strain relationship. This is a clear evidence of the robustness of the proposed model.

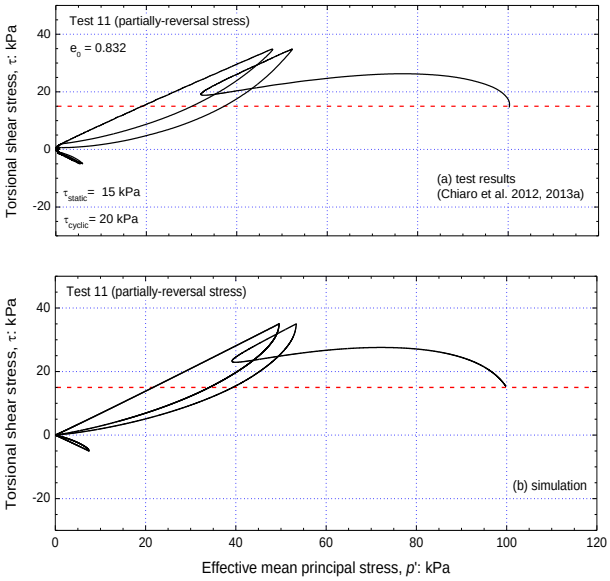

Figure 9 Measured and simulated effective stress paths for Test 11

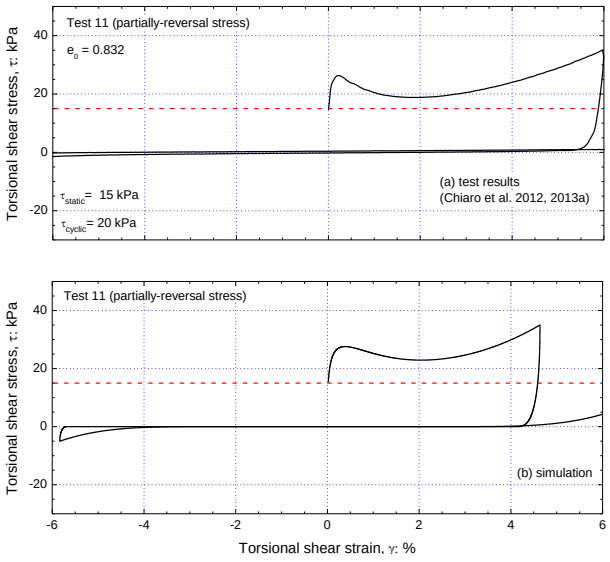

Figure 10 Measured and simulated stress-strain relationships for Test 11

5.3 Progressive accumulation of residual deformation under non-reversal stress loading

Results of a non-reversal torsional shear test (D_r = 45.3%; e_0 =0.829; τ_{static} = 20 kPa and τ_{cyclic} = 16 kPa) are shown in Figures 11*a* and 12*a*. Despite gradual Δu generation, full liquefaction state is not reached ($\Delta u/p$' ≈ 90%). However, progressive development of large shear strain larger than 7.5% occurred in a few cycles of loafing. Model simulations shown in Figures 11*b* and 12*b* are clearly in agreement with the experimental results, confirming that the proposed model is able to reproduce sand behavior also under non-reversal stress conditions.

5.4 No-liquefaction under non-reversal stress loading

Figures 13*a* and 14*a* refer to the cyclic undrained response of a medium dense Toyoura sand specimen undergoing non-reversal stress conditions (D_r = 47.7%; e_0 =0.820; τ_{static} = 15 kPa and τ_{cyclic} = 10 kPa). In this test, despite undergoing 100 cycles of loading, only very limited Δu is generated (i.e. ($\Delta u/p$' ≈ 20%). Significantly, it is

also observed that the extent of shear strain is very small (≈ 0.2 %). This type of no liquefaction and no failure cyclic behavior has rarely been reported in the literature for sandy soils. It has to be mentioned that, this test was specifically carried out in the laboratory to support the numerical simulations (Figures 13*b* and 14*b*). In fact, this uncommon behavior was first observed by chance in a series of numerical simulations.

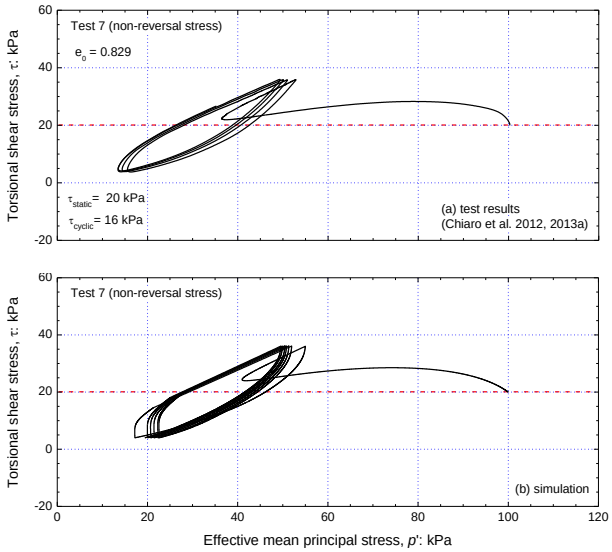

Figure 11 Measured and simulated effective stress paths for Test 7

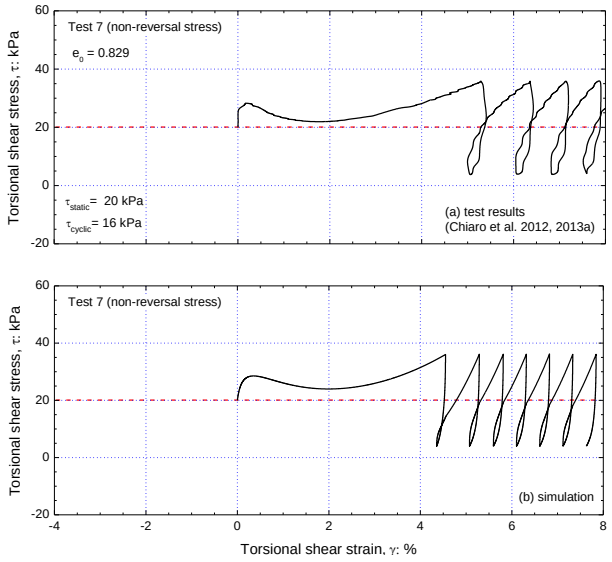

Figure 12 Measured and simulated stress-strain relationships for Test 7

5.5 Effects of fabric on Toyoura sand failure modes

Laboratory observations have shown that the soil fabric (i.e. spatial arrangement of sand particles and associated voids) plays an important role on Toyoura sand elastic properties (De Silva, et al. 2006) and response to cyclic loading and its failure modes (Sze and Yang, 2014). Therefore, the fabric should be regarded as a state parameter as important as density and confining stress in describing soil behavior. However, due to the lack of a complete experimental database for hollow cylindrical Toyoura specimens prepared with different methods (e.g. moist tamping or water sedimentations, that would provide different soil fabrics) to use for model calibration and validation, the fabric effects were not integrated in the proposed model. This would need to be addressed by future studies.

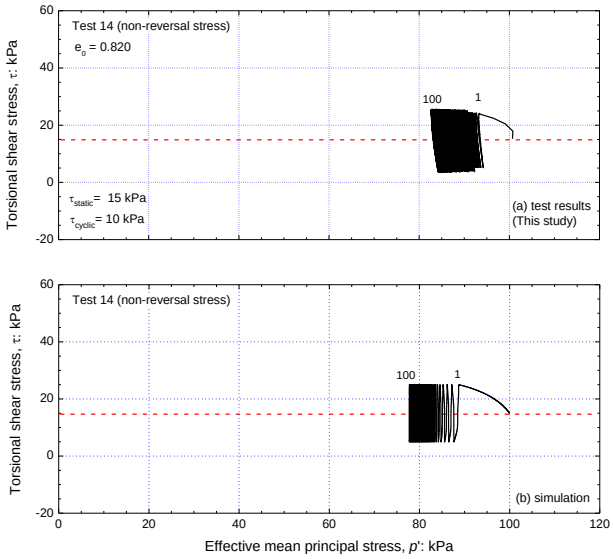

Figure 13 Measured and simulated effective stress paths for Test 14

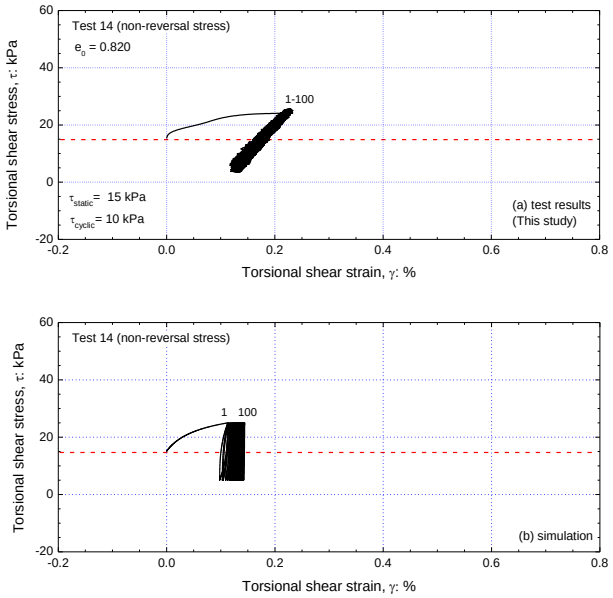

Figure 14 Measured and simulated stress-strain relationships for Test 14

6. SUMMURY AND CONCLUSIONS

A robust state-dependent cyclic model to describe the behavior of saturated sands subjected to undrained cyclic torsional simple shear loading with initial static shear was presented in this paper. The model is based on an extended GHE approach and a state-dependent cyclic bi-linear stress-dilatancy relationship. It is able to simulate the stress-strain soil behavior over a wide range of densities and confining pressure by using a single set of 20 model soil parameters. By comparing the numerical simulations with the experimental results, it is demonstrated that the proposed model was able to describe pre- and post-liquefaction behavior of Toyoura sand, capturing the salient features of the effective stress paths and stress-strain relationships, under partially-reversal shear stress loading condition. As well, progressive accumulation of residual shear strain observed under non-reversal shear stress loadings was also well simulated. Moreover, the model predictions revealed that under non-reversal shear stress conditions, medium-dense Toyoura sand may also experience no liquefaction and no shear strain development

depending on the combination of initial static shear and cyclic shear. This latter behavior was later confirmed by experimental work.

7. LIST OF SYMBOLS

d_1, d_2: dilatancy parameters
dp': effective mean stress increment
$d\gamma$, $d\gamma^e$, $d\gamma^p$: total, elastic and plastic shear strain increments
$d\varepsilon_{vol}$: total volumetric strain increment
$d\varepsilon^e_{vol}$, $d\varepsilon^p_{vol}$: elastic and plastic volumetric strain increments
e: current void ratio
e_0: initial void ratio (i.e. at the end of consolidation)
e_{ic}: void ratio at reference isotropic confining stress
$f(e)$, $f(e_0)$: current and initial void ratio functions
$f(e_{ic})$: void ratio function at reference isotropic confining stress
G, G_0: current and initial shear moduli
G_{ic}: shear modulus at reference isotropic confining stress
G_n: small strain shear stiffness parameter
K, K_0: current and initial bulk moduli
K_{ic}: bulk modulus at reference isotropic confining stress
K_m: compressibility parameter
m, n: soil parameter for bulk modulus and shear modulus
N_d: gradient of stress-dilatancy relation
p', p_0': current and initial effective mean stresses
p_{ic}': reference confining stress
x, y: normalized plastic shear strain and normalized stress ratio
γ^p, γ_{ref}: plastic and reference shear strains
δ, F_1, F_2: drag function and parameters
Δu: excess pore water pressure
α, β, Γ, $\xi_{1(0)}$, $\xi_{1(\infty)}$, $\xi_{2(0)}$, $\xi_{2(\infty)}$: GHE parameters
$\xi_{1(x)}$, $\xi_{2(x)}$: strain-dependent GHE fitting parameters
$(\tau/p')_{max}$, ρ_1, ρ_2: peak stress ratio and its parameters
τ, $d\tau$:: shear stress and shear stress increment
$(\tau/p')_{PTL}$: stress ratio at phase transformation

8. REFERENCES

Arangelovski, G., and Towhata, I. (2004) "Accumulated deformation of sand with initial shear stress and effective stress state lying near failure conditions". Soils and Foundations, 44, Issue 6, pp 1-16.

Byrne, P. M. (1991) "A cyclic shear-volume coupling and pore pressure model for sand". Proceedings of Int. Conference on Recent Advances in Geotechnical Earthquake Engineering and Soil Dynamics, Paper 1.

Castro, G., and Poulus, S. J. (1977) "Factors affecting liquefaction and cyclic mobility". Journal of the Geotechnical Engineering Division, ASCE, 103, Issue GT6, pp 501-551.

Chiaro, G., Koseki, J., and Sato, T. (2012) "Effects of initial static shear on liquefaction and large deformation properties of loose saturated Toyoura sand in undrained cyclic torsional shear". Soils and Foundations, 52, Issue 3, pp 498-510.

Chiaro, G., Kiyota, T., and Koseki, J. (2013a) "Strain localization characteristics of loose saturated Toyoura sand in undrained cyclic torsional shear tests with initial static shear". Soils and Foundations, 53, Issue 1, pp 23-34.

Chiaro, G., Koseki, J. and De Silva, L. I. N. (2013b) "A density- and stress-dependent elasto-plastic model for sands subjected to monotonic torsional shear loading", Geotechnical Engineering, SEAGS, 44, Issue 2, pp 18-26.

Chiaro, G., Koseki, J., and De Silva, L. I. N. (2013c) "An elasto-plastic model for liquefiable sands subjected to torsional shear loadings". Springer Series in Geomechanics and Geoengineering, pp 519-526.

Chiaro, G., Koseki, J., De Silva, L. I. N., and Kiyota, T. (2015) "Modeling the monotonic undrained torsional shear response of loose and dense Toyoura sand". JGS Special Publication, 2, Issue 9, pp 407-410.

De Silva, L. I. N., Koseki, J., and Sato, T. (2006) "Effects of different pluviation techniques on deformation property of hollow cylinder sand specimens". Proceedings of Int. Symposium on Geomechanics and Geotechnics of Particulate Media, Ube, Yamaguchi, Japan, pp 29-33.

De Silva, L. I. N., and Koseki, J. (2012) "Modelling of sand behavior in drained cyclic shear". Advances in Transportation Geotechnics II, Miura et al. (eds.), CRC Press, pp 686-691.

De Silva, L. I. N., Koseki, J, Chiaro, G., and Sato, T. (2015) "A stress-strain description for saturated sand under undrained cyclic torsional shear loading". Soils and Foundations, 55, Issue 3, pp 559-574.

De Silva, L. I. N., Koseki, J., Wahyudi, S., and Sato, T. (2014) "Stress-dilatancy relationships of sand in the simulation of volumetric behavior during cyclic torsional shear loadings". Soils and Foundations, 54, Issue 4, pp 845-858.

Georgiannou, V. N., Tsomokos, A., and Stavrou, K. (2008) "Monotonic and cyclic behaviour of sand under torsional loading", Geotechnique, 58, Issue 2, pp 113-124.

Hardin, B. O. and Richart, F. E. (1963) "Elastic wave velocities in granular soils". Journal of Soil Mechanics and Foundation Division, ASCE, 89, Issue SM1, pp 33-65.

Hight, D. W., Gens, A., and Symes, M. J. (1983) "The development of a new hollow cylinder apparatus for investigating the effects of principal stress rotation in soils". Geotechnique, 33, pp 355-383.

HongNam, N. (2004) "Locally measured quasi-elastic properties of Toyoura sand in cyclic triaxial and torsional loadings". Ph.D. Thesis, Dept. of Civil Eng., University of Tokyo, Japan.

HongNam, N., and Koseki, J. (2005) "Quasi-elastic deformation properties of Toyoura sand in cyclic triaxial and torsional loadings". Soils and Foundations, 45, Issue 5, pp 19-38.

Hyodo, M., Murata, H., Yasufuku, N., and Fujii, T. (1991) "Undrained cyclic shear strength and residual shear strain of saturated sand by cyclic triaxial tests". Soils and Foundations, 31, Issue 3, pp 60-76.

Ishihara, K., Tatsuoka, F., and Yasuda, S. (1975) "Undrained deformation and liquefaction of sand under cyclic stresses". Soils and Foundations, 15, Issue 1, pp 29-44.

Iwasaki, T., Tatsuoka, F., and Takagi, Y. (1978) "Shear modulus of sand under cyclic torsional shear loading". Soils and Foundations, 18, Issue 1, pp 39-56.

Kiyota, T., De Silva, L. I. N., Sato, T., and Koseki, J. (2006) "Small strain deformation characteristics of granular materials in torsional shear and triaxial tests with local deformation measurements". Soil stress-strain behavior: measurement, modeling and analysis, Ling et al. (eds.), pp 557-566.

Kiyota, T., Sato, T., Koseki, J., and Mohammad, A. (2008) "Behavior of liquefied sands under extremely large strain levels in cyclic torsional shear tests". Soils and Foundations, 48, Issue 5, pp 727-739.

Koseki, J., Yoshida, T., and Sato, T. (2005) "Liquefaction properties of Toyoura sand in cyclic torsional shear tests under low confining stress". Soils and Foundations, 45, pp 103-113.

Lee, K. L. and Seed, H. B. (1967) "Dynamic strength of anisotropically consolidated sand". Journal of Soil Mechanics and Foundation Division, ASCE, 93, Issue SM5, pp 169-190.

Masuda, T., Tatsuoka, F., Yamada, S. and Sato. T. (1999) "Stress-strain behavior of sand in plane strain compression, extension and cyclic loading tests". Soils and Foundations, 39, pp 31-45.

Nishimura, S., and Towhata, I. (2004) "A three-dimensional stress-strain model of sand undergoing cyclic rotation of principal stress axes". Soils and Foundations, 44, Issue 2, pp 103-116.

Oka, F., Yashima, A., Tateishi, Y., Taguchi, Y., and Yamashita, S. (1999) "A cyclic elasto-plastic constitutive model for sand considering a plastic-strain dependence of the shear modulus". Geotechnique, 49, Issue 5, pp 661-680.

Pradhan, T. B. S., Tatsuoka, F., and Sato, Y. (1989) "Experimental stress-dilatancy relations of sand subjected to cyclic loadings". Soils and Foundations, 29, Issue 1, pp 45-64.

Rowe, P. W. (1962) "The stress-dilatancy relation for static equilibrium of an assembly of particles in contact". Proceedings of Royal Society of London, Series A, 269, pp 500-527.

Shahnazari, H., and Towhata, I. (2002) "Torsion shear tests on cyclic stress-dilatancy relationship of sand". Soils and Foundations, 42, issue 1, pp 105-119.

Sivathayalan, S., and Ha, D. (2011) "Effect of static shear stress on the cyclic resistance of sands in simple shear loading". Canadian Geotechnical Journal, 48, Issue 10, pp 1471–1484.

Sze, H. Y., and Yang, J. (2014) "Failure modes of sand in undrained cyclic loading: impact of sample preparation". Journal of Geotechnical and Geoenvironmental Engineering, ASCE, 140, Issue 1, pp 152-169.

Taiebat, M., and Dafalias, Y. F. (2010) "Simple yield surface expression appropriate for soil plasticity". International Journal of Geomechanics, ASCE, 10, Issue 4, pp 161-169.

Tatsuoka, F., Jardine, R. J., Lo Presti, D., Di Benedetto, H., and Kodata, T. (1997) "Characterizing the pre-failure deformation properties of geomaterials". Proceedings of 14th Int. Conference on Soil Mechanics and Foundations Engineering, Hamburg, Germany, 4, pp 2129-2164.

Tatsuoka, F., Masuda, T., Siddquee, M. S. A., and Koseki, J. (2003) "Modeling the stress-strain relations of sand in cyclic plane strain loading". Journal of Geotechnical and Geoenvironmental Engineering, ASCE, 129, Issue 6, pp 450-467.

Tatsuoka, F., Muramatsu, M., and Sasaki, T. (1982) "Cyclic undrained stress-strain behavior of dense sands by torsional simple shear stress". Soils and Foundations, 22, pp 55-70.

Tatsuoka, F., and Shibuya, S. (1992) "Deformation characteristics of soils and rocks from field and laboratory tests". Proceedings of 9th Asian Regional Conference on Soil Mechanics and Foundation Engineering, Bangkok, Thailand, 2, pp 101-170.

Vaid, Y. P., and Chern, J. C. (1983) "Effects of static shear on resistance to liquefaction". Soils and Foundations, 23, pp 47-60.

Vaid, Y. P., and Finn, W. D. L. (1979) "Static shear and liquefaction potential". Journal of the Geotechnical Engineering Division, ASCE, 105, pp 1233-1246.

Vaid, Y. P., Stedman, J. D., and Sivathayalan, S. (2001) "Confining stress and static shear effects in cyclic liquefaction". Canadian Geotechnical Journal, 38, Issue 3, pp 580-591.

Umar, M., Chiaro, G., and Kiyota, T. (2016) "On the influence of initial static shear on large deformation behavior of very loose Toyoura sand in undrained cyclic torsional shear tests". JGS Special Publication, 4, Issue (2), pp 17-22.

Yang, J., and Sze, H. Y. (2011) "Cyclic behavior and resistance of saturated sand under non-symmetrical loading conditions". Geotechnique, 61, Issue 1, pp 59-73.

Yoshimi, Y., and Oh-oka, H. (1975) "Influence of degree of shear stress reversal on the liquefaction potential of saturated sand". Soils and Foundations, 15, Issue 3, pp 27-40.